

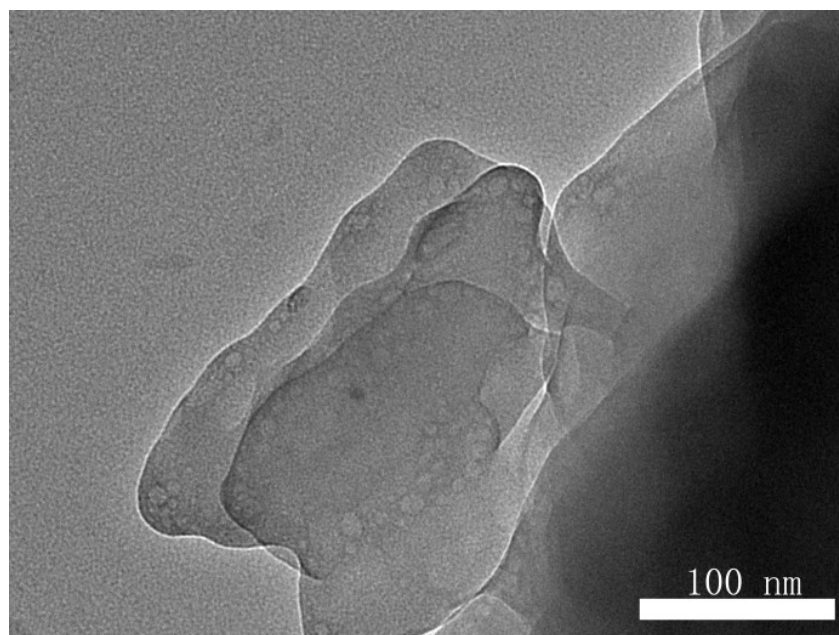
supporting information

**A high-capacity and long-life aqueous rechargeable zinc battery using porous metal–organic coordination polymers nanosheets cathode**

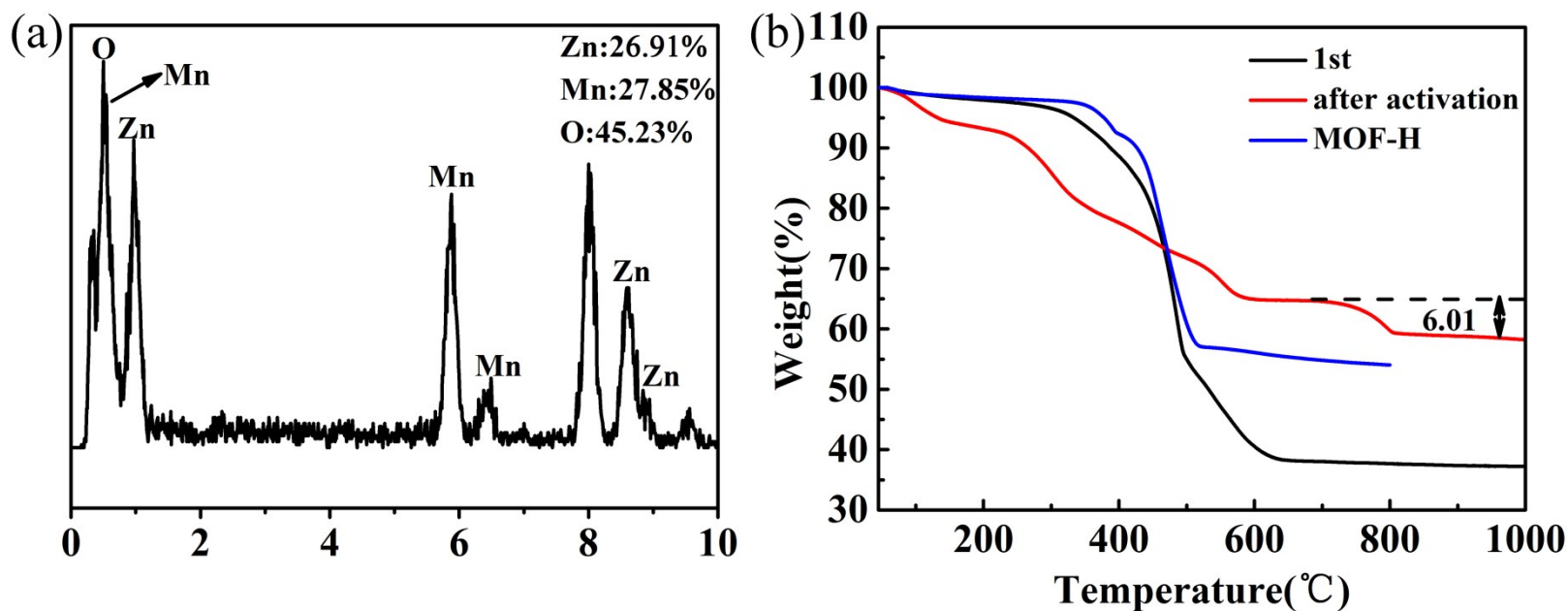
Shan Wu <sup>a</sup>, Yi-Fan Wang <sup>a</sup>, Wei-Liang Liu <sup>\*,a</sup>, Man-Man Ren <sup>a</sup>, Fan-Gong Kong <sup>\*,b</sup>, Shou-Juan Wang <sup>b</sup>, Xin-Qiang Wang <sup>c</sup>, Hui Zhao <sup>a,d</sup>, Jin-Ming Bao <sup>a</sup>

Table. S1 Existing materials for neutral ARZB

Cathode	Electrolyte	Rate performance	Cycling performance	Ref
$\text{Zn}_3\text{V}_2\text{O}_7(\text{OH})_2 \cdot 2\text{H}_2\text{O}$	1 M $\text{ZnSO}_4$	213 mAh $\text{g}^{-1}$ at 50 mA $\text{g}^{-1}$ 76 mAh $\text{g}^{-1}$ at 3000 mA $\text{g}^{-1}$	68% (300, 200mA $\text{g}^{-1}$ )	1
$\text{VS}_2$	$\text{ZnSO}_4$	159.1 mAh $\text{g}^{-1}$ at 0.1 A $\text{g}^{-1}$ 136.8 mAh $\text{g}^{-1}$ at 0.5 A $\text{g}^{-1}$	98% (200, 0.5A $\text{g}^{-1}$ )	2
$\alpha\text{-MnO}_2$	1 M $\text{ZnSO}_4$ + 0.1 M $\text{MnSO}_4$	285 mAh $\text{g}^{-1}$ at C /3 161 mAh $\text{g}^{-1}$ at 5 C	92% (5000, 5C)	3
$\text{Zn}_{0.25}\text{V}_2\text{O}_5 \cdot n\text{H}_2\text{O}$	1 M $\text{ZnSO}_4$	282 mAh $\text{g}^{-1}$ at 0.3 A $\text{g}^{-1}$ 223 mAh $\text{g}^{-1}$ at 4.5 A $\text{g}^{-1}$	80% (1000, 2.4 A $\text{g}^{-1}$ )	4
$\text{ZnHCF}$	1 M $\text{ZnSO}_4$	81 mAh $\text{g}^{-1}$ at 0.06 A $\text{g}^{-1}$ 32.3 mAh $\text{g}^{-1}$ at 1.2 A $\text{g}^{-1}$	81% (100, 0.06A $\text{g}^{-1}$ )	5
$\text{Zn}_{1/3}\text{Ni}_{1/3}\text{Mn}_{2/3}\text{O}_2$	1 M $\text{ZnSO}_4$	113.7 mAh $\text{g}^{-1}$ at 0.05 C 19.4 mAh $\text{g}^{-1}$ at 0.2 C	92.3% (30, 0.05C)	6
$\text{V}_{0.95}\text{Al}_{0.05}\text{O}_{1.52}(\text{OH})_{0.77}$	1 M $\text{ZnSO}_4$	156 mAh $\text{g}^{-1}$ at 0.015 A $\text{g}^{-1}$	81% (50, 0.015A $\text{g}^{-1}$ )	7



**Figure S1.**Transmission electron microscope of MOCP-H.



**Figure S2.** TEM-EDX (a) and thermogravimetric (TG) analyses (b) of MOCP-H after activation.

TEM-EDX confirms the elemental weight of Mn is 27.85 % (Fig. S2a). TG analysis reveals 6.01 % weight loss in the temperature range 600 to 1000 °C, which was due to the transition from  $\text{Mn}_2\text{O}_3$  to  $\text{Mn}_3\text{O}_4$  with the reduce of O elemental (Fig. S2b)<sup>8,9</sup>. The weight of  $\text{MnO}_2$  is about 36.06 %, so the weight of Mn elemental (27.81 %) deduced from the TG analysis is consistent with TEM-EDX result.

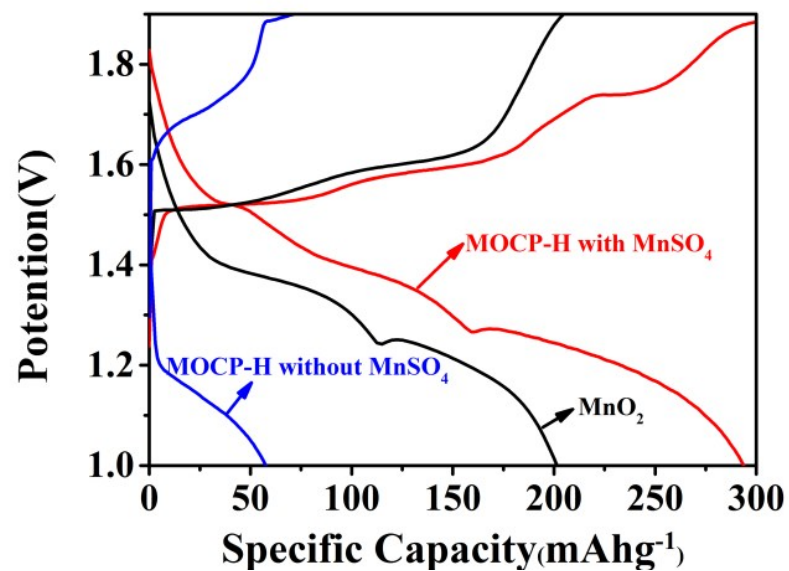


**Figure S3.** The discharge/charge profiles of the MOCP-H with  $\text{MnSO}_4$ , MOCP-H without  $\text{MnSO}_4$  and  $\text{MnO}_2$  at a current density of  $60 \text{ mA g}^{-1}$  in the potential range of 1.0-1.9 V (vs.  $\text{Zn/Zn}^{2+}$ ).

The MOCP-H electrode in  $\text{ZnSO}_4/\text{MnSO}_4$  solution electrolyte exhibits a higher discharge capacity ( $294 \text{ mAh g}^{-1}$ ) than that of the MOCP-H electrode in  $\text{ZnSO}_4$  solution electrolyte ( $57.5 \text{ mAh g}^{-1}$ ), which could be attributed to the formation of  $\text{MnO}_2$ . The discharge capacity of  $\text{MnO}_2$  is  $201.5 \text{ mAh g}^{-1}$ .

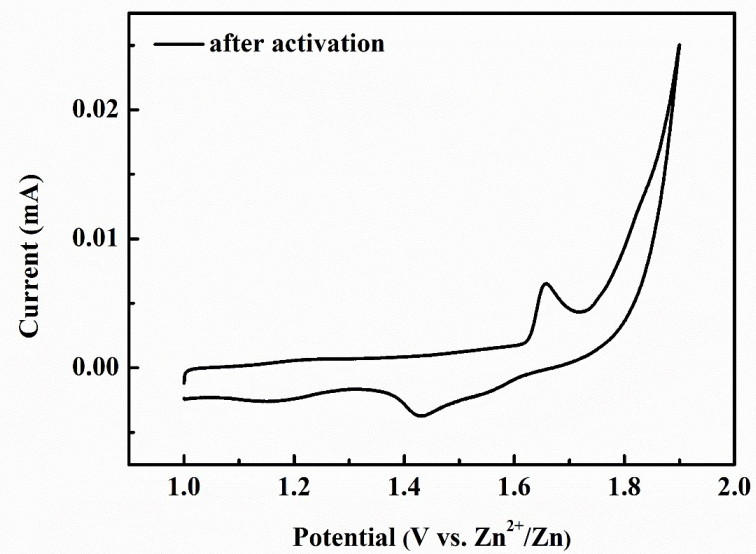


**Figure S4.** Cyclic voltammetric curves of MOCP-H in  $\text{ZnSO}_4$  at a scan rate of  $0.1 \text{ mV s}^{-1}$  in a potential range of 1.0-1.9 V (vs.  $\text{Zn}/\text{Zn}^{2+}$ ). On the continuous cycles, reveals one oxidation peak at 1.69 V and one reduction peaks at 1.41V.

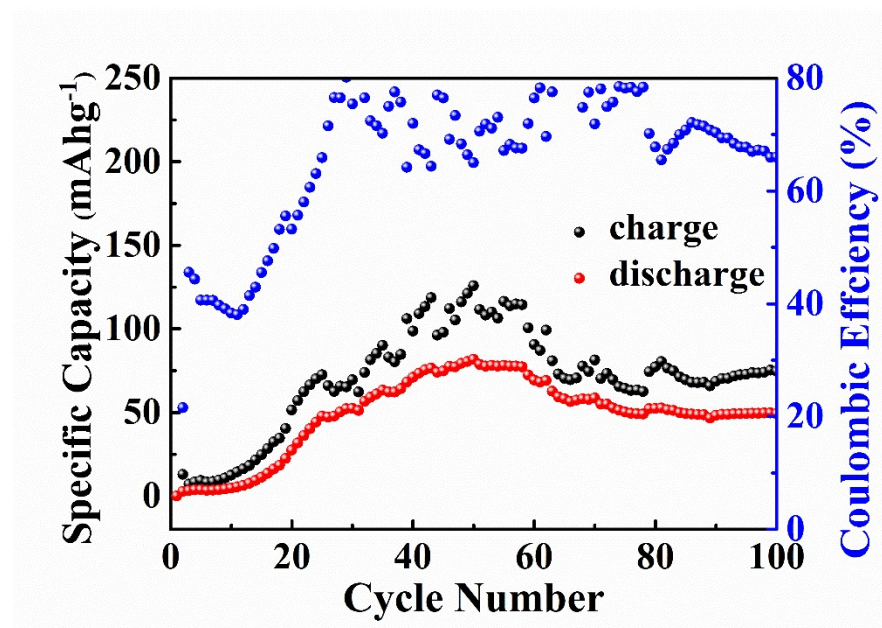


**Figure S5.** MOCP-H in  $\text{ZnSO}_4$  at  $60 \text{ mAh g}^{-1}$  in a potential range of 1.0-1.9 V. The cells were activated in the first 50 cycles.

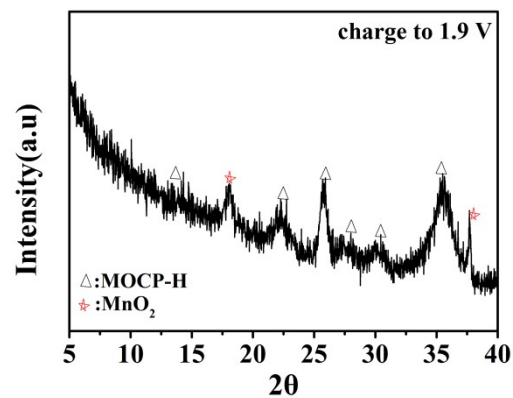


**Figure S6.** XRD curve of charge.

The XRD peaks of the MOCP-H were weak in Fig. 5 when charging to 1.9 V, which can be ascribed to the influence of MnO<sub>2</sub>. But, some characteristic peaks of the MOCP-H were still existing when charging to 1.9 V.

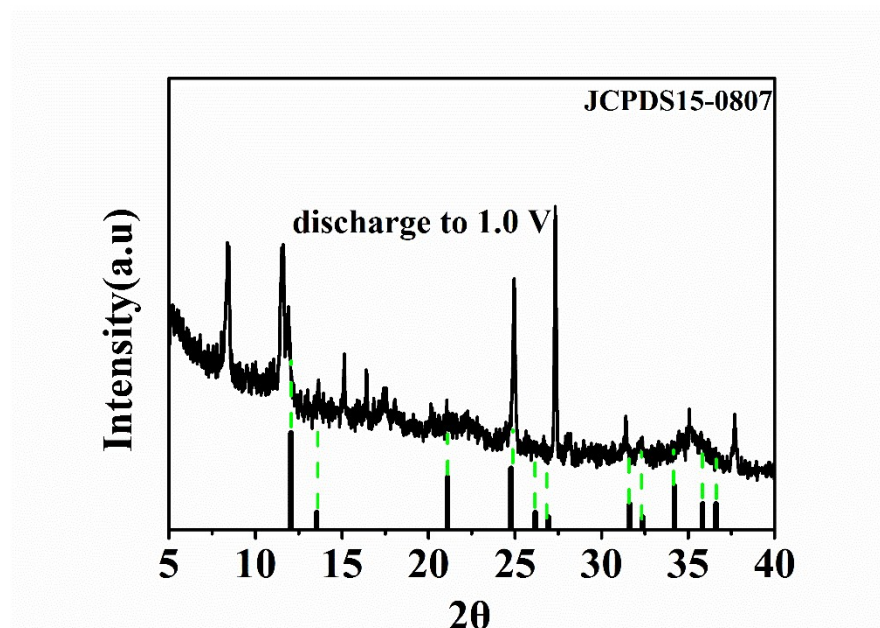


**Figure S7.** XRD curve of discharge.

XRD peaks of the MOCP-H when discharging to 1.0 V, the individual XRD curve of discharge shows only two types of peaks which from  $\text{ZnMn}_3\text{O}_7 \cdot 3\text{H}_2\text{O}$  and MOCP-H. The MOCP solid can be totally hydrolyzed back to metal salt and organic acid in discharge, and terephthalic acid becomes the only solid product detected by XRD<sup>8</sup>. The XRD peak of  $\text{H}_2\text{BDC}$  was not found in charge, and the MOCP-H solid can't be hydrolyzed back to metal salt and organic acid.



## References

1. C. Xia, J. Guo, Y. Lei, H. Liang, C. Zhao and H. N. Alshareef, *Advanced materials*, 2018, **30**.
2. P. He, M. Yan, G. Zhang, R. Sun, L. Chen, Q. An and L. Mai, *Advanced Energy Materials*, 2017, **7**, 1601920.
3. H. Pan, Y. Shao, P. Yan, Y. Cheng, K. S. Han, Z. Nie, C. Wang, J. Yang, X. Li, P. Bhattacharya, K. T. Mueller and J. Liu, *Nature Energy*, 2016, **1**, 16039.
4. D. Kundu, B. D. Adams, V. Duffort, S. H. Vajargah and L. F. Nazar, *Nature Energy*, 2016, **1**, 16119.
5. L. Zhang, L. Chen, X. Zhou and Z. Liu, *Advanced Energy Materials*, 2015, **5**, 1400930.
6. Y. Zhang, K. Cheng, K. Ye, Y. Gao, W. Zhao, G. Wang and D. Cao, *Electrochimica Acta*, 2015, **182**, 971-978.
7. J. H. Jo, Y.-K. Sun and S.-T. Myung, *Journal of Materials Chemistry A*, 2017, **5**, 8367-8375.
8. Z.-Y. Yuan, Z. Zhang, G. Du, T.-Z. Ren and B.-L. Su, *Chemical Physics Letters*, 2003, 378, 349-353.
9. A. M. Joseph and R. T. Kumar, *Materials Research Express*, 2018, 5, 014002.
10. L. Huang, H. Wang, J. Chen, Z. Wang, J. Sun, D. Zhao and Y. Yan, *Microporous and Mesoporous Materials*, 2003, **58**, 105-114.